

An Optimal Controller for Load Frequency Control in Multi-Area Deregulated power system

In this paper, an optimal controller for load frequency control in multi area power system in deregulated environment is suggested. The controller is designed and analyzed for LFC in multi-area power system while each area consists of different multi-sources such as hydro, thermal reheat and non-reheat. To solve LFC problem, a PID controller is designed while its parameters are tuned using nature inspired Social Spider Optimization algorithm. For each area, local PID controller is designed which minimize the frequency deviation of that area and tie line power exchange while various contracts commitments are taken care. It is also observed that load change, disturbance and uncertainty in system parameters have no effect on the performance of the designed controller. The performance of suggested controller is studied and analyzed in all possible contracts in deregulated power market. The controller is simulated in MATLAB/SIMULINK. The superiority of proposed approach has been shown by comparing dynamic performance of designed PID using SSO with PSO and DE. The results are compared for various performance measures like overshoot, undershoot, settling time, frequency deviation and deviation in tie line power. The designed controller is also compared with existing fractional PID and ANFIS controller. On comparison it is found that designed controller is robust and gives better results in all aspects.

Keywords: LFC; PID controller; deregulated environment; social spider optimization; Area control error

Article history: Received 26 May 2018, Accepted 11 February 2019

1. Introduction

Power system generally face power mismatch between the scheduled generation and load demand which leads to variation in frequency. The increase/decrease of load causes decrease/increase the frequency from the nominal value. Under normal conditions, this frequency deviation is small and is controllable while if this frequency deviation goes beyond certain limits then it directly impacts the power system operation and system reliability. To maintain frequency in an area within its specified limits, load frequency control (LFC) is done in generating stations which makes a balance between load demand and generation. As power system has several generators units which are connected to each other with the help of tie lines for exchange of power between them in order to enhance fault/load tolerance. In an interconnected power system, whenever load demand changes it results variation in both frequency and tie line power exchange. Therefore LFC problem in an interconnected system becomes more complex as in this case LFC is related directly with maintenance of frequency and minimization of tie line exchange error between various generating units at scheduled values so that frequency deviation in each area is maintained and it's within its limits [1].As

* Corresponding author: Damanjeet Kaur, Assistant Professor of Electrical and Electronic Engineering (EEE), UIET, Panjab University, Chandigarh, India, E-mail: damanee@pu.ac.in.

¹ Alireza Sina, Faculty member of ACECR, Research scholar in UIET, Panjab University, Chandigarh, India, E-mail: sina@acecr.ac.ir.

² Damanjeet Kaur, Assistant Professor of Electrical and Electronic Engineering (EEE), UIET, Panjab University, Chandigarh, India

conventional electrical utilities moved from vertical integrated structure to a deregulated power system which consists of generation, transmission and distribution companies and independent system operator (ISO). In deregulated power system, power is exchanged between GENCOs and DISCOs and contracts of power exchange are signed between them. These contracts between GENCO and DISCO may be bilateral, poolco or sometimes there is violation of these contracts. In bilateral DISCO can take power from any generator may be some other area also while in poolco DISCO has to take power from generators of its own area. In an interconnected deregulated power system with different energy sources and multi region, sudden change in load demand in any area lead to change in power generation, which changes the frequency and contractual energy exchange between different areas. For successful operation of power system, frequency and contractual energy exchange between various areas should be constant. During contract violations made by the DISCOs, LFC reschedules the generations of each GENCO to re-establish the frequency and minimize the unscheduled power flows [2]. So the main objective of LFC is to maintain the system frequency at nominal value and contractual energy exchange between different areas [3, 4].

The transient deviations and steady state error is minimized to zero in advance. To meet these objectives researchers developed various classical optimal [5, 6] and intelligent controllers [7-11]. Authors solved LFC problem for single area [12], multi-area in conventional [13-16] and deregulated environment [17-19]. Authors considered LFC problem in deregulated environment for multi-source like non-reheat [20-23] reheat [20, 21] and hydro [20] sources.

To solve LFC, most of the researchers used PID controllers because of its accuracy and high speed. As the performance of PID is directly increased by its parameters tuning. Therefore authors used AI based techniques like fuzzy [9, 24], GA [7, 8], PSO [9, 12, 25], Honey Bee [26, 27], DE [28, 29], Firefly [24, 30, 31] and SSO [11] for tuning of parameters in order to optimize the gain of controllers. Authors implemented PID [17], ANFIS [20] and fractional order PID [21-23] to solve LFC problem.

In this paper SSO optimization technique is used to tune the parameters of PID controller to solve LFC of multi area deregulated power systems. The superiority of the proposed approach is shown by comparing the results with DE and PSO optimization algorithms in deregulated power system. Deregulated power system contain seven units those are non-reheat, reheat and hydro in three areas. In order to better demonstrate the proposed method, the control system is evaluated for three models of existing scenarios. Poolco, bilateral and contract violation scenario. Results are shown in tables and figures. Load changes, disturbances and uncertainty in the system parameters are also considered.

2. System Modeling and LFC in Deregulated Environment

In a deregulated power market in order to create balance between GENCOs and DISCOs, contracts are signed between companies based on rules and relationships. These contract could be bilateral, Poolco or a combination of both [6, 32]. In the Poolco contract, each DISCO meets its power requirement only from the generators of its own area. But In the bilateral contract, each DISCO can deal with any GENCO in any area [6, 33]. In the present study, three areas are considered in deregulated power system. Area-1 consists of 3-thermal generations, while Area-2 and 3 have 2 generations of type hydro and thermal respectively.

GENCO1, GENCO2, GENCO3, DISCO1, DISCO2 in area-1, GENCO4, GENCO5, DISCO3, DISCO4 in Area-2 and GENCO6, GENCO7 and DISCO5 are located in area 3. The relationship between GENCOS and DISCOS, is derived using DPM matrix. It can be expressed as given below:

$$DPM = \begin{bmatrix} cpf_{11} & cpf_{12} & cpf_{13} & cpf_{14} & cpf_{15} \\ cpf_{21} & cpf_{22} & cpf_{23} & cpf_{24} & cpf_{25} \\ cpf_{31} & cpf_{32} & cpf_{33} & cpf_{34} & cpf_{35} \\ cpf_{41} & cpf_{42} & cpf_{43} & cpf_{44} & cpf_{45} \\ cpf_{51} & cpf_{52} & cpf_{53} & cpf_{54} & cpf_{55} \\ cpf_{61} & cpf_{62} & cpf_{63} & cpf_{64} & cpf_{65} \\ cpf_{71} & cpf_{72} & cpf_{73} & cpf_{74} & cpf_{75} \end{bmatrix} \quad (1)$$

In this matrix, the number of columns represent the total number of DISCO present in multiple areas. The number of rows represent the total number of GENCO in all specified areas. Each element of this matrix represents GENCO participation factor for DISCO power supply. So cpf_{ij} is defined as GENCO i contract participation factor for DISCO j for total power supply. In Matrix DPM, equation $\sum_{i=1}^N cpf_{ij} = 1$ should always be correct until each DISCO receive its power requirement from generators in different areas. With the help of DPM, Power produced and Power Planned of each generator, for transferring electrical energy between various regions, can be obtained. Power Requirements of DISCO j can be defined as ΔP_{Lj} . Total power requirement of a DISCO in area i is the sum of contracted power and contract violation.

$$\Delta P_{Di} = \Delta P_{L1} + \Delta P_{L2} + \dots + \Delta P_{Ln} + \Delta P_{Lviolation} \quad (2)$$

Total power generated is given as:

$$\Delta P_{gi} = \sum_{j=1}^n cpf_{ij} \Delta P_{Lj} \quad (3)$$

Power committed between regions i and j as:

$$\Delta P_{tie,ij,schedule} = (\text{Demand of DISCOs in Area } j \text{ from GENCOs in Area } i) - (\text{Demand of DISCOs in Area } i \text{ from GENCOs in Area } j) \quad (4)$$

As in area-1, 3-Generators and 2 DISCOs are present while in area-2, 2-Generators and 2 DISCOs are present. To calculate the tie-line power scheduled between Area 1 and 2 can be mathematically expressed as:

$$\Delta P_{tie,12,schedule} = \sum_{i=1}^3 \sum_{j=3}^4 cpf_{ij} \Delta P_{ij} - \sum_{i=4}^5 \sum_{j=1}^2 cpf_{ij} \Delta P_{ij} \quad (5)$$

Similarly, $\Delta P_{tie,23,schedule}$ and $\Delta P_{tie,13,schedule}$ are calculated.

To control the power exchange between regions i and j , the difference between tie line power scheduled and actual power is calculated as:

$$\Delta P_{tie,ij,error} = \Delta P_{tie,ij,actual} - \Delta P_{tie,ij,schedule} \quad (6)$$

In equation (6), $\Delta P_{tie,ij,actual}$ is amount of actual power transferred between regions i and j that is given by:

$$\Delta P_{tie,ij,actual} = \frac{T_{ij} 2\pi}{S} (\Delta f_i - \Delta f_j) \quad (7)$$

In order to control the frequency and the power scheduled between different areas, area control error (ACE) signal is calculated. In each area it is specified and sent to the controller for the same area. This signal can be represented as follows:

$$ACE = \sum_j (\Delta P_{tie,ij,error} + B_i \Delta f_i) \tag{8}$$

In equation (8) B_i is the base frequency coefficient area of i and Δf_i is the frequency difference of area i .

3. Design of Controllers

3.1. PID Controller

The PID controller is one of the easiest and, at the same time, the most reliable control method in the power industry. Therefore, it has been widely applied in the industry. The PID controller makes the system stable by adding zeros and poles to it. To improve the performance of the PID controller, its parameters must be accurately calculated. The deregulated power system that has been studied here includes three area and seven sources. In this paper, each power deregulated area is controlled by a PID controller. Therefore, in order to obtain optimal values for the parameters of the PID controller, the transmission performance of each region must be calculated independently. The transfer functions obtained from each area are connected to a PID controller and the frequency stability for step function. The parameters of the PID controller are also compared with other evolutionary algorithms like SSO, DE and PSO. After obtaining optimal parameters in each area. All three areas are considered together in deregulated power system for frequency control and tie line power exchange. The developed model is simulated in MATLAB environment under various contracts (Poolco, Bilateral and violation). The model of PID controller parameters optimization is shown in Fig 1 [34, 35].

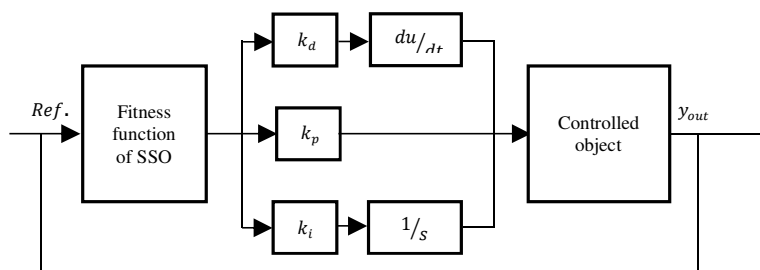


Fig. 1. Optimization of the PID controller

3.2. Social Spider Optimization

Social spider algorithm (SSA) is proposed by Yu and Li [36] to solve optimization problem. SSO is a swarm intelligence algorithm which is inspired from the behaviors of the spiders (male and female). Following are the steps of the algorithm: [37].

Step 1: Choose N number of colony in search space and define the number of male N_{male} and female N_{female} spiders in the entire colony S based on Eq. 9.

$$N_{male} = N - N_{female} , \quad N_{female} = floor[(0.9 - rand * 0.25)N] \tag{9}$$

Where $rand$ stands for a random number which falls within the range of $[0,1]$ and $floor(.)$ indicates the mapping between a real and an integer numbers.

Step 2: Initialize stochastically the female and male members and compute the mating radius according to Eq. 10.

$$r = \frac{\sum_{j=1}^n (p_j^{high} - p_j^{low})}{2n} \tag{10}$$

$$f_{i,j}^0 = p_j^{low} + rand(0, 1)(p_j^{high} - p_j^{low}), m_{k,j}^0 = p_j^{low} + rand(0, 1)(p_j^{high} - p_j^{low})$$

Once the new spider is formed, it is compared with the worst spider of the colony. If the new spider is better, the worst spider is replaced by the new one. Where f_{ij} is the j th parameter of the i th female spider position.

Step 3: Calculate the weight of each spider in colony S through Eq. 11.

$$w_i = \frac{J(S_i) - worst_S}{best_S - worst_S} \quad (11)$$

Where $J(S_i)$ denotes the fitness value acquired through the evaluation of the spider position S_i with regard to the objective function $J(.)$.

Step 4: Move female spiders according to the female cooperative operator modelled as in Eq.12. Since the final movement of attraction or repulsion depends on several random phenomena, the selection is modeled as a stochastic decision. For this operation, a uniform random number r_m is generated within the range $[0, 1]$. If r_m is smaller than a threshold PF, an attraction movement is generated; otherwise, a repulsion movement is produced.

$$f_i^{k+1} = \begin{cases} f_i^k + \alpha V_i bc_i (S_c - f_i^k) + \beta V_i bb_i (S_b - f_i^k) + \delta(rand - 0.5) & \text{with probability PF} \\ f_i^k - \alpha V_i bc_i (S_c - f_i^k) - \beta V_i bb_i (S_b - f_i^k) + \delta(rand - 0.5) & \text{with probability } 1 - PF \end{cases} \quad (12)$$

Calculate $V_i bc_i$ and $V_i bb_i$

if ($r_m < PF$)

$$f_i^{k+1} = f_i^k + \alpha V_i bc_i (S_c - f_i^k) + \beta V_i bb_i (S_b - f_i^k) + \delta(rand - 0.5)$$

else if

$$f_i^{k+1} = f_i^k - \alpha V_i bc_i (S_c - f_i^k) - \beta V_i bb_i (S_b - f_i^k) + \delta(rand - 0.5)$$

end

end

Where α, β and δ and rand are random numbers which fall within the range of $[0, 1]$.

Step 5: Similarly move male spiders according to the male cooperative operator as expressed in Eq.13.

$$m_i^{k+1} = \begin{cases} m_i^k + \alpha V_i bf_i (S_f - m_i^k) + \delta(rand - 0.5) & \text{if } W_{N_{female}} + i > W_{N_{female}} + m \\ m_i^k + \alpha \left(\frac{\sum_{h=1}^{N_{male}} m_h^k W_{N_{female}} + h}{\sum_{h=1}^{N_{male}} W_{N_{female}} + h} - m_i^k \right) & \text{if } W_{N_{female}} + i \leq W_{N_{female}} + m \end{cases} \quad (13)$$

for ($i = 1; i < N_m + 1; i++$)

calculate $V_i bf_i$

$$\text{if } (W_{N_f} + i > W_{N_f} + m) \text{ then } m_i^{k+1} = m_i^k + \alpha V_i bf_i (S_f - m_i^k) + \delta(rand - 0.5)$$

$$\text{else if } m_i^{k+1} = m_i^k + \alpha \left(\frac{\sum_{h=1}^{N_{male}} m_h^k W_{N_{female}} + h}{\sum_{h=1}^{N_{male}} W_{N_{female}} + h} - m_i^k \right)$$

end

end

Where S_f indicates the nearest female spider to the male individual.

Step 6: Perform the mating operation. Mating in a social-spider colony is performed by dominant males and the female members. In the mating process, the weight of each involved spider defines the probability of influence for each individual into the new brood. The spiders holding a heavier weight are more likely to influence the new product, while elements with lighter weight have a lower probability.

Step 7: Check again whether the stopping criterion is satisfied. If yes, the algorithm terminates; otherwise, return to Step 3.

Different to other evolutionary algorithms, in SSOA, each individual spider is modelled by taking its gender into account. This design allows incorporating computational mechanisms to avoid critical flaws and incorrect exploration exploitation trade-off. In order to show how the SSOA performs [38].

4. Simulation and Results

The present system (Figure 2 in Appendix 1) is simulated in Sim/MATLAB for automatic generation control in a three-area deregulated power system while thermal and hydro generators are present. The simulation results for all possible contracts in the deregulated power market is obtained using PID controller while PID parameters are optimized using SSO. Parameters for three-area in deregulated power system are given in Table 3 (in Appendix 1). epf_k , is the k_{th} generator economic participation factor [39]. In this paper, generators economic participation factors are assumed as: $epf_1 = 0.3$, $epf_2 = 0.32$, $epf_3 = (1 - (epf_1 + epf_2)) = 0.38$, $epf_4 = 0.7$, $epf_5 = (1 - epf_4) = 0.3$, $epf_6 = 0.6$, $epf_7 = (1 - epf_6) = 0.4$ respectively. In all contracts, power required by each DISCO is considered equal to 0.05 pu.MW.

4.1. Scenario 1: Poolco Based Transactions

In this case, each DISCO meets its power demand only from GENCOS of its own area. DPM matrix is built which shows the relationship between GENCOS and DISCOS for this contract, as: In the present scenario three area system is studied.

$$DPM = \begin{bmatrix} 0.4 & 0.22 & 0 & 0 & 0 \\ 0.3 & 0.33 & 0 & 0 & 0 \\ 0.3 & 0.45 & 0 & 0 & 0 \\ 0 & 0 & 0.6 & 0.8 & 0 \\ 0 & 0 & 0 & 0.4 & 0.2 & 0 \\ 0 & 0 & 0 & 0 & 0 & 0.6 \\ 0 & 0 & 0 & 0 & 0 & 0.4 \end{bmatrix}$$

Figures 3 and 4 are related to change in frequency in three areas and tie lines power - exchanged between different areas. The controller is designed using the SSO algorithms in terms of undershoot (US), overshoot (OS) and settling time (ST). When load is increased in three area with 0.05 pu MW. To meet increased load demand, generators of each area produce more power as: $\Delta P_{G_{11}} = 0.031$, $\Delta P_{G_{21}} = 0.0315$, $\Delta P_{G_{31}} = 0.0375$, $\Delta P_{G_{42}} = 0.07$, $\Delta P_{G_{52}} = 0.03$, $\Delta P_{G_{63}} = 0.03$ and $\Delta P_{G_{73}} = 0.02$ respectively. Fig. 3, 4 are obtained for the simulated model show the change in frequency in all areas and tie lines power exchange between various areas. On analyzing the frequency deviation of each area it is clear from Fig.3 (a), (b) and (c) that frequency deviation in each area settles to zero in steady state in less than 4 sec. while actual tie line power deviation response for the three area system is zero as shown in Fig.4 (a), (b) and (c) respectively.

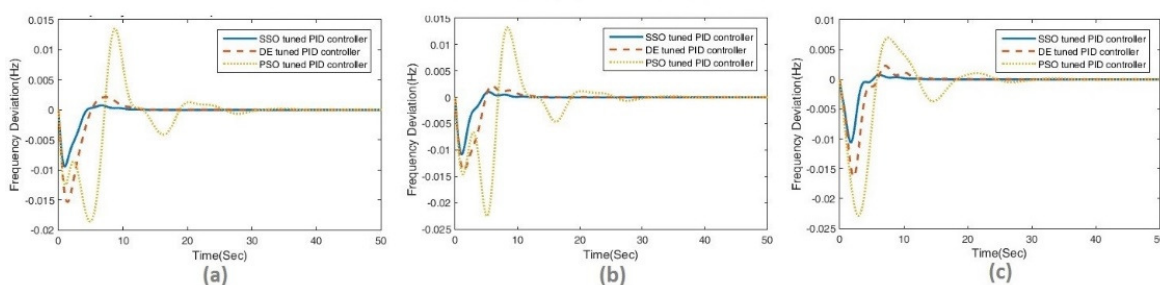


Fig3. (a), (b) and (c) frequency deviation response of area1,2,3 in scenario 1

On comparing the results with DE and PSO it is found that DE and PSO take more settling time nearly 12 sec. and 20 sec. respectively as compared to SSO. The detailed transient dynamic response using suggested PID controller is mentioned in Table 4 (Appendix). The DPM matrix in this contract can be theoretically calculated using equation 3. Figures 5 is related to generator power output response.

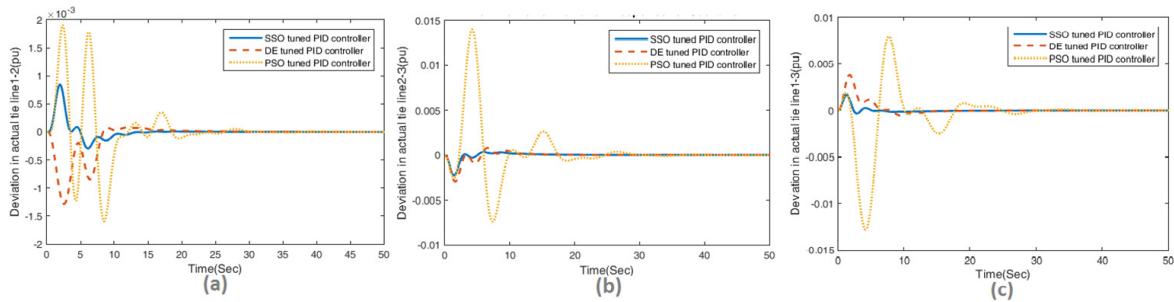


Fig4. (a), (b), (c) Tie line power deviation response between different lines in scenario 1

4.2. Scenario 2: Bilateral Transactions

In these types of contracts, each DISCO can get power from GENCOS of its own area or from another area. The DPM matrix for the given contract can be expressed as given below:

$$DPM = \begin{bmatrix} 0.2 & 0.15 & 0.1 & 0 & 0.2 \\ 0.25 & 0.2 & 0 & 0.1 & 0.15 \\ 0.1 & 0 & 0.3 & 0.25 & 0.15 \\ 0.3 & 0.15 & 0.3 & 0.25 & 0.2 \\ 0 & 0.2 & 0 & 0.15 & 0.2 \\ 0.15 & 0.2 & 0.15 & 0.15 & 0 \\ 0 & 0.1 & 0.15 & 0.1 & 0.1 \end{bmatrix}$$

The results of designed controller and DE and PSO based are compared in terms of OS, US and ST (by taking Bond 0.05%) which clearly indicates that suggested controller has more appropriate response than DE and PSO algorithms.

For the increased load demand, the power output of each generator is calculated theoretically in steady state which results are $\Delta P_{G_1} = 0.0325$, $\Delta P_{G_2} = 0.035$, $\Delta P_{G_3} = 0.04$, $\Delta P_{G_4} = 0.06$, $\Delta P_{G_5} = 0.0275$, $\Delta P_{G_6} = 0.0325$, $\Delta P_{G_7} = 0.0225$ respectively.

On analyzing the frequency deviation of each area it is clear from Fig.6 (a), (b) and (c) that frequency deviation in each area settles to zero in steady state in less than 12 sec. It is clear from Fig.7 that in simulated model generators show the consistent results with theoretical values. Using equation 4 and DPM Matrix, power exchanged between various areas are calculated as $\Delta P_{tie12} = 0.005$, $\Delta P_{tie23} = -0.0075$ and $\Delta P_{tie13} = 0.0025$. Again simulated results coverage to the calculated values, as shown in Fig.8. On comparing the results of SSO tuned PID controller, DE and PSO, it is clear from Fig.7 and Fig.8 that SSO tuned PID has better accuracy. The detailed results of undershoot, over shoot and settling time using SSO, DE and PSO mentioned in Table 6 and Table 7 (Appendix) respectively.

4.3. Scenario 3: Contract Violation

Sometimes, DISCOS demand more power than the committed in contracts. In such situations this excess uncommitted power must be supplied from the GENCOs of the same area. Suppose a DISCOS in area-2 demand 0.01pu more power than the committed contract then total power demand of DISCOS in area-2 will be as given below:

$$\Delta P_{D_2} = (\text{load of DISCO3}) + (\text{load of DISCO4}) + 0.01 = 0.05 + 0.05 + 0.01 = 0.11$$

Total DISCOS power in area-1 and area-3 will remain unchanged. So $\Delta p_{d_1} = 0.1$, $\Delta p_{d_3} = 0.05$, DPM matrix is considered as in scenario-1. Power produced by generators in first and third areas remain unchanged. The amount of power demand by DISCOS in area-2 should be provided by generators in the same area i.e. Area-2 as follows:

$$_{-}(4, Violuton) = [\Delta P_G]_{-4} + [epf]_{-4} \times [\Delta P]_{-violation} = 0.077, [\Delta P_G]_{-}(5, Violuton) = [\Delta P_G]_{-5} + [epf]_{-5} \times [\Delta P]_{-violation} = 0.033$$

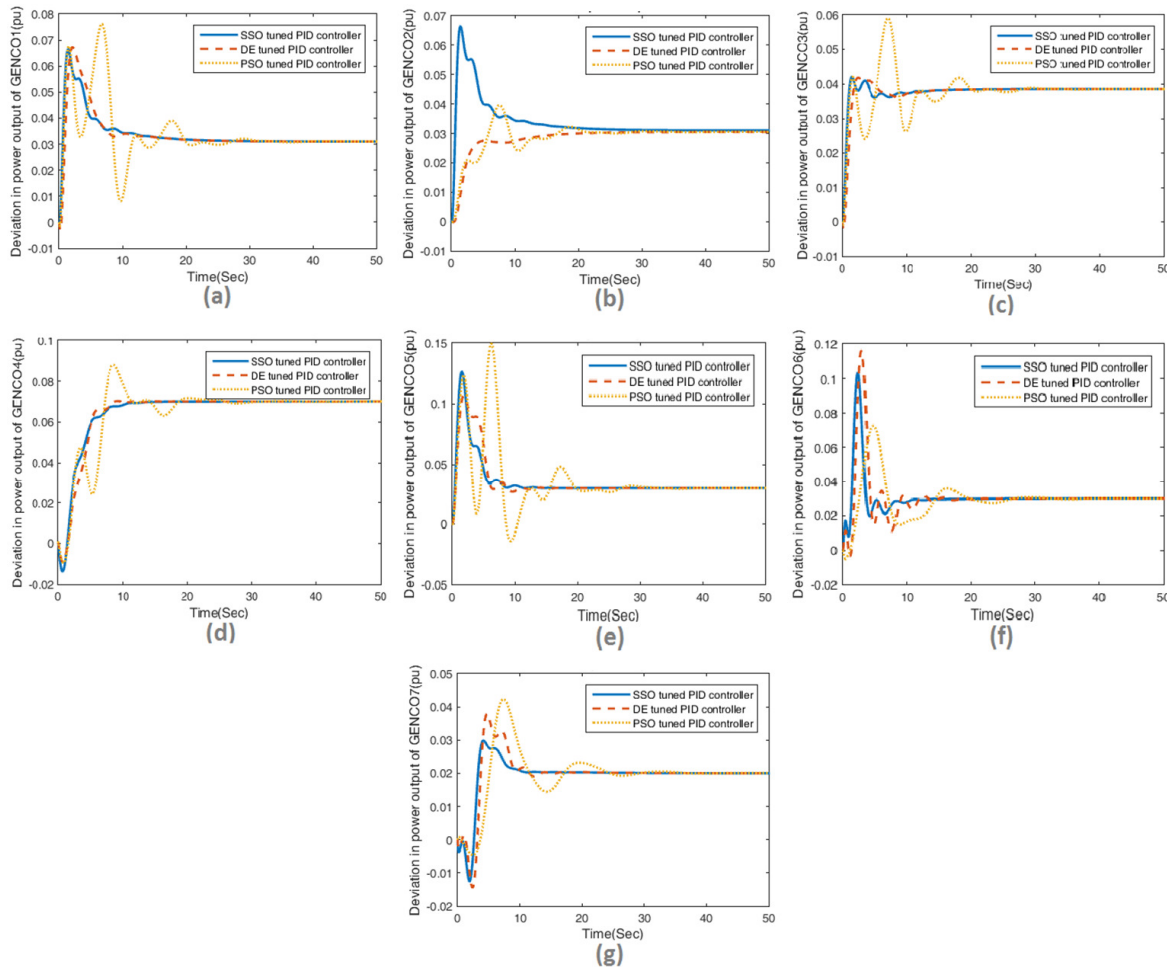


Fig5. (a), (b), (c), (d), (e), (f) and (g) generator power output response in scenario1

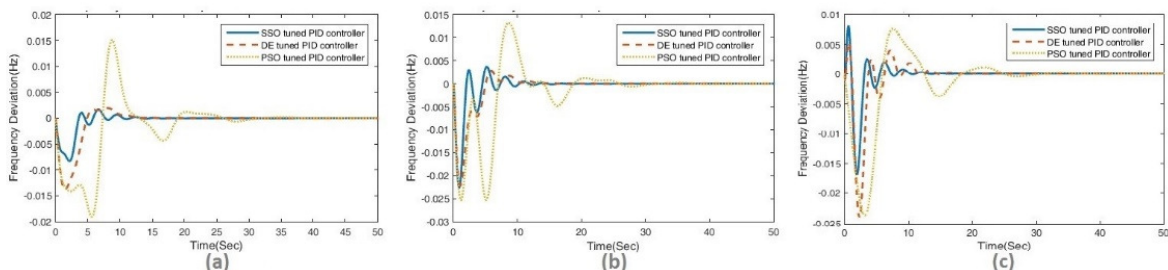


Fig6. (a), (b) and (c) frequency deviation response of area 1,2,3 in scenario2

The controller dynamic response for this using the SSO is shown in Fig. 9 and 10 which clearly indicates that there is no change in power demand in area-1 and area-3 as in scenario-2 except in area-2. SSO algorithm based PID controller in terms of OS, US and ST (with Band 0.05%) yields more appropriate response than DE and PSO algorithms. The complete

transient dynamic response characteristics are tabulated in Table 4 (Appendix). The power output of each generator is shown in the Fig.11. The value in steady state, is same as with the calculated values. For better understanding evaluation of controller against sudden load changes, system dynamic response is studied in detail as mentioned in Tables 5 and 6 (Appendix 2) respectively.

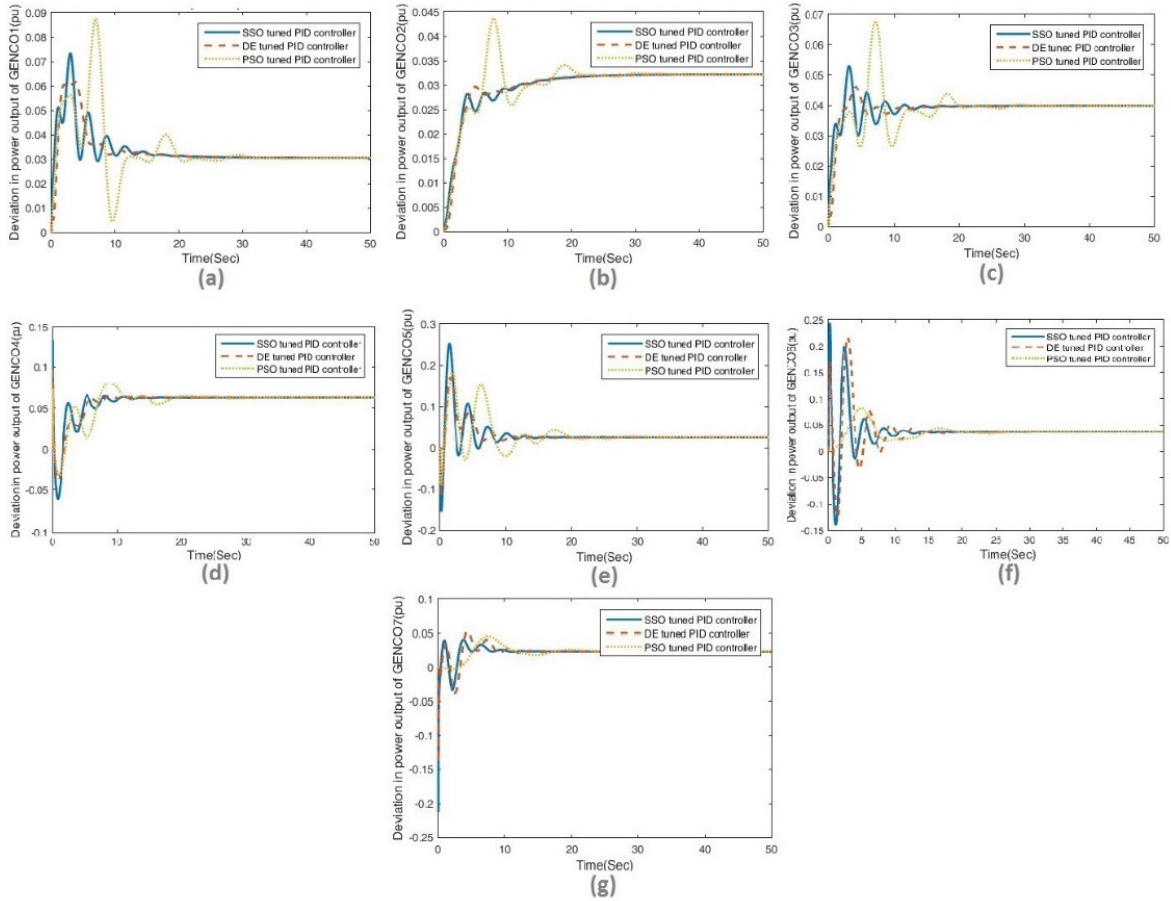


Fig7. (a), (b), (c), (d), (e), (f) and (g) generators power output response in scenario 2

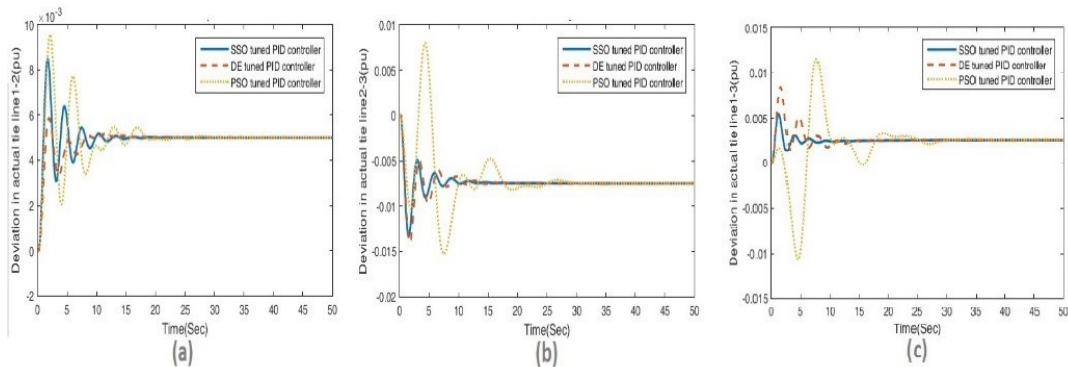


Fig.8. (a), (b) and (c) tie line power deviation response between different lines in scenario2

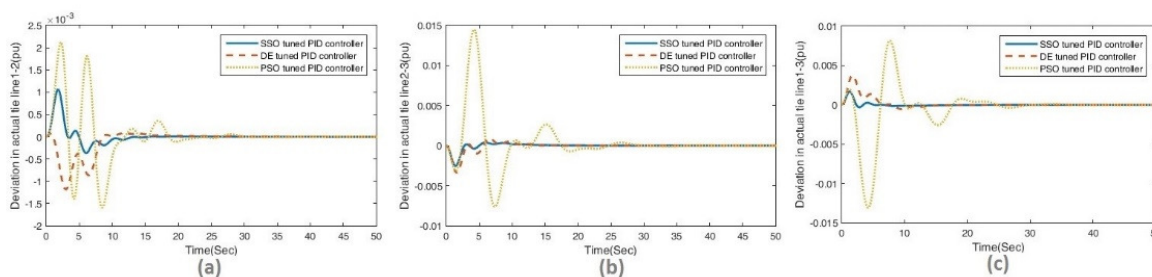


Fig 9. (a), (b) and (c) frequency deviation responses of area 1,2,3 in scenario-3

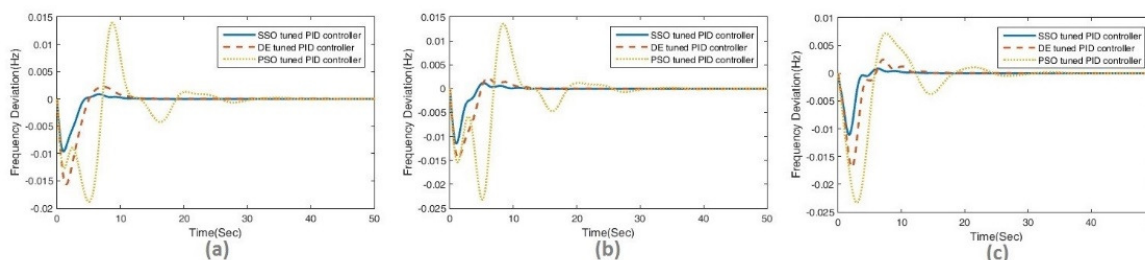


Fig 10. (a), (b) and (c) tie line power deviation responses between different lines in Scenario-3

For this study tables 5 and 6 clearly show that OS, US and ST increases with increase in load. It is assumed that DISCOs total power requirement in each region, change between -50 to +50% (with band ± 0.05). The results are also compared with DE and PSO in Table 5 and 4. It is clear from results that SSO performs better than DE and PSO in all scenarios. Hence it is clear that designed controller has satisfactory performance against load changes.

4.4. Controller Performance against Changes in System Parameters

In order to evaluate the performance of the controller against possible changes to system parameters tables 7 and 8 (Appendix 2) are provided. In accordance with the tables on the parameters T_{GH} , T_{RS} , T_{RH} , T_r and T_t at a rate of -25 to +25% have been changed and compared to their nominal values. The tabulated results show that parameters Δf_1 , Δf_2 , Δf_3 , ΔP_{tie12} , ΔP_{tie23} and ΔP_{tie13} , OS, US and ST (by taking band 0.05%) in each contracts are in an acceptable range. When system parameters are changed, the controller has good dynamic performance against frequency and tie line power exchanges.

4.5. Comparison with Existing Controllers

The performance of designed controller is compared with existing ANFIS [20], fractional PID [21, 22] and fuzzy PID controllers [40] for scenario 3. The results are tabulated in Table 1 and 2 for undershoot, overshoot, tie line power exchange and settling time in two and three areas systems respectively. On comparison, it is clear from Table 1 and 2 that proposed controller's performance is better than ANFIS, fractional PID and fuzzy controllers in terms of undershoot, overshoot, frequency deviation, tie line power exchange and settling time (Table 2) in all areas Hence it is clear from the results that suggested controller is better performing in 2-area as well as in 3-area in all cases.

Table 1. Comparison of US and OS for scenario 3*

Method	US (10^{-3})						OS (10^{-3})					
	Δf_1	Δf_2	Δf_3	ΔP_{Tie1-2}	ΔP_{Tie2-3}	ΔP_{Tie1-3}	Δf_1	Δf_2	Δf_3	ΔP_{Tie1-2}	ΔP_{Tie2-3}	ΔP_{Tie1-3}
ANFIS [20]	67.9	51	32.5	37	9	29.8	29.1	13	17.5	90.8	49	11.66
FOPID [21]	27	19.5	-	15	-	-	7.6	1.8	-	55	-	-
FOPID [22]	73	12	-	-	-	-	-	-	-	-	-	-
2DOFPID [23]	65.31	17.12	-	12.45	-	-	0	0	-	0	-	-
fuzzy-DE- PID [40]	246	142	-	16	-	-	17	22	-	13.8	-	-
Proposed methods SSO-PID	9.6	11.4	11.1	0.3	2.5	0.3	8	1.2	0.8	1	0.4	1.6

Table 2. Comparison of Settling time for scenario 3

Method	Areas	ST (Sec.)						
		Δf_1	Δf_2	Δf_3	ΔP_{Tie1-2}	ΔP_{Tie2-3}	ΔP_{Tie1-3}	
ANFIS [20]	3	15	13	12	8	9	13	
FOPID [21]	2	17	12	-	23	-	-	
FOPID [22]	2	6	8	-	-	-	-	
2DOFPID [23]	2	8.536	10.88	-	21.65	-	-	
Adaptive fuzzy-DE- PID [40]	2	4.39	7.56	-	5.13	-	-	
Proposed methods SSO-PID	3	10	8.61	7.28	2.68	2.43	2.76	

5. Conclusion

In this paper an intelligent controller in deregulated environment is designed. An extensive analysis of proposed LFC system controller in the deregulated environment is done when execution of the contracts Poolco, bilateral and contract violation are taken into account. Results clearly show that PID controller adjust frequency deviation and Tie line power exchange quickly.

In order to show superiority of PID designed controller using SSO algorithm, the results of the dynamic behavior of parameters such as frequency and power tie line changes are compared with the results of the DE and PSO algorithms. Results proved that SSO algorithm has better overshoot, undershoot and settling time in all possible contracts as compared to DE and PSO. Furthermore simulations results show that the proposed algorithm is not affected by changes in load and uncertainty in the system parameters and the controller has satisfactory dynamic operation. To validate the proposed controller the performance of SSO-PID is compared with existing fractional PID, fuzzy PID and ANFIS controllers also. The comparative results conclude the robustness and quick response of the suggested controller.

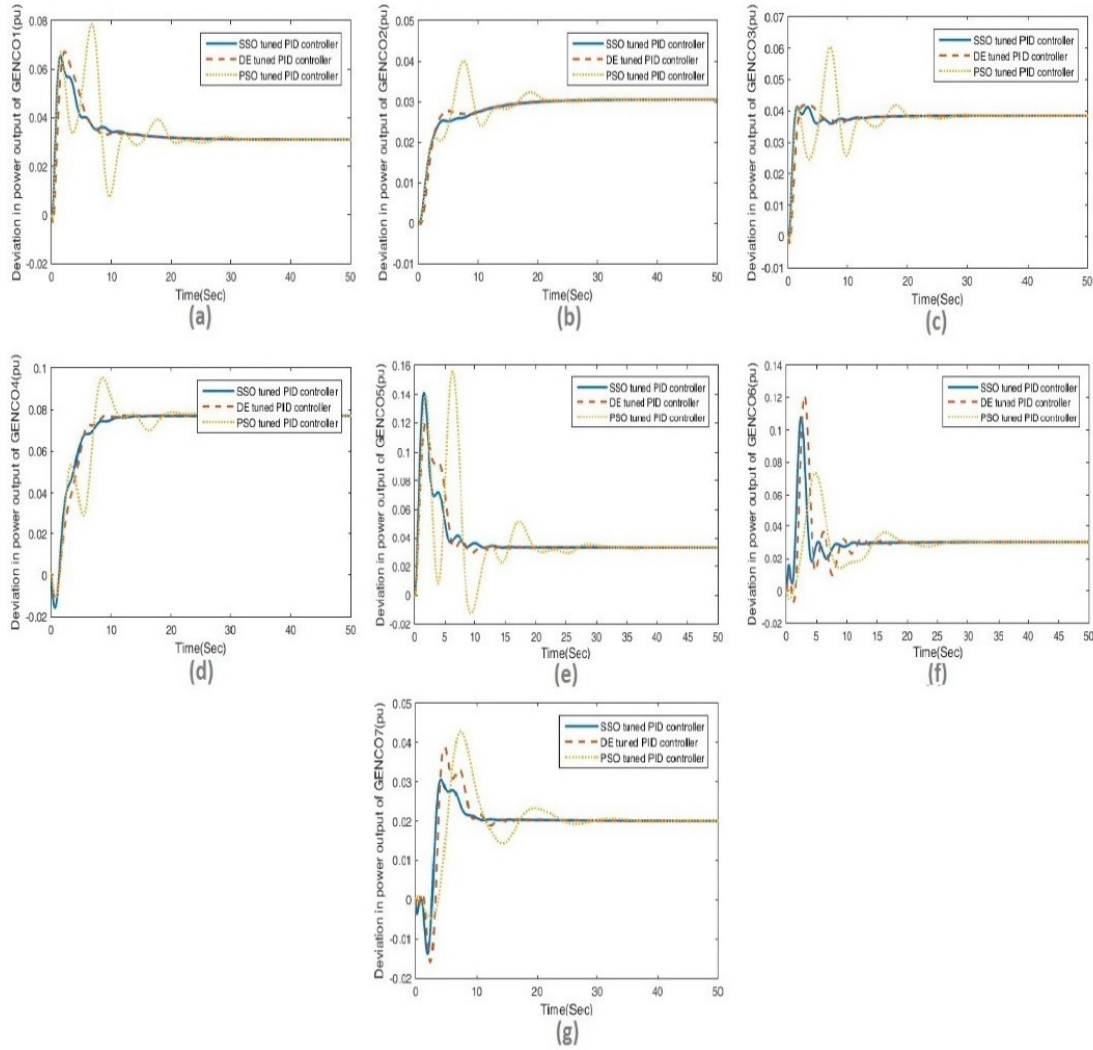


Fig11. (a), (b), (c), (d), (e), (f) and (g) generators power output response in scenario-3

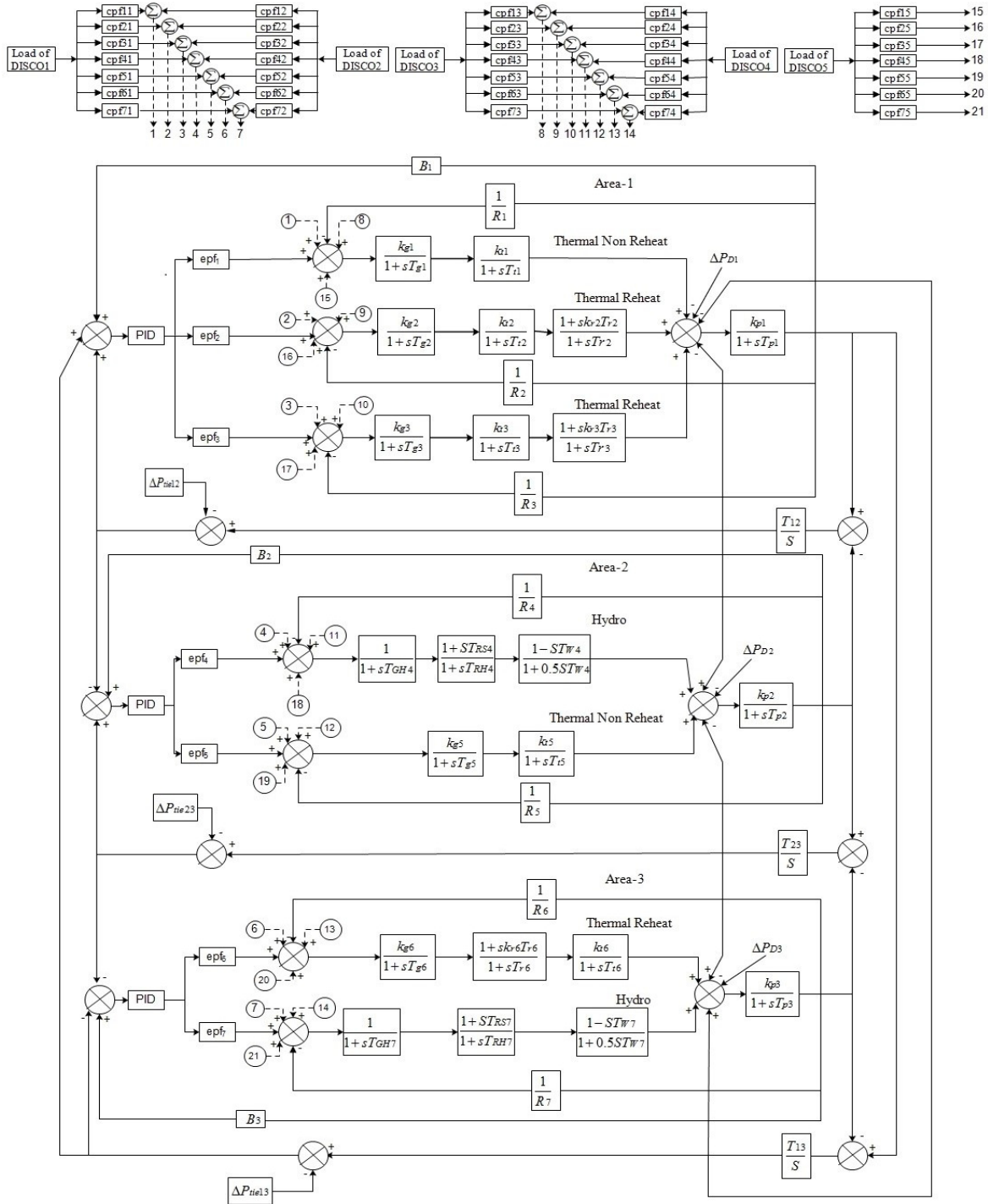
Appendix 1. Parameters Values and System Model

Table 3. Power system parameters

Area1	
$T_{g1} = 0.08 s, T_{t1} = 0.35 s, R_1 = 0.3333 \frac{HZ}{pu} . MW, k_{g1} = k_{t1} = 1$	
$T_{g2} = 0.875 s, T_{t2} = 0.375 s, k_{r2} = 0.3113, T_{r2} = 10.6 s, R_2 = 0.32 \frac{HZ}{pu} . MW, k_{g2} = k_{t2} = 1$	
$T_{g3} = 0.08 s, T_{t3} = 0.3 s, k_{r3} = 0.5, T_{r3} = 10 s, R_3 = 0.33 \frac{HZ}{pu} . MW, k_{g3} = k_{t3} = 1$	
$k_{p1} = 20 \frac{HZ}{pu} . MW, T_{P1} = 120 s, B_1 = 0.532 \frac{pu}{MW} . HZ$	
Area 2	
$T_{GH4} = 0.1 s, T_{RH4} = 10 s, T_{RS4} = 0.513 s, T_{W4} = 1 s, R_4 = 0.32 \frac{HZ}{pu} . MW, k_{g4} = k_{t4} = 1$	
$T_{g5} = 0.075 s, T_{t5} = 0.38 s, R_5 = 0.2963 \frac{HZ}{pu} . MW, k_{g5} = k_{t5} = 1$	
$k_{p2} = 20 \frac{HZ}{pu} . MW, T_{P2} = 120 s, B_2 = 0.495 \frac{pu}{MW} . HZ$	
Area 3	
$T_{g6} = 0.07 s, T_{t6} = 0.36 s, k_{r6} = 0.33, T_{r6} = 10 s, R_6 = 0.289 \frac{HZ}{pu} . MW, k_{g6} = k_{t6} = 1$	

$$T_{GH7} = 0.015 \text{ s}, T_{RH7} = 8.75 \text{ s}, T_{RS7} = 0.1513 \text{ s}, T_{W7} = 1.5 \text{ s}, R_7 = 0.3077 \frac{\text{HZ}}{\text{pu}} \cdot \text{MW}, k_{g7} = k_{t7} = 1$$

$$k_{p2} = 20 \frac{\text{HZ}}{\text{pu}} \cdot \text{MW}, T_{P2} = 120 \text{ s}, B_2 = 0.542 \frac{\text{pu}}{\text{MW}} \cdot \text{HZ}, T_{12} = T_{23} = T_{13} = 0.543 \text{ pu/HZ}$$



Appendix 2.

Table 4. Comparison of transient characteristics for scenario 1, 2 and 3

Ctrl.	Par.	Peak overshoot (OS)			Peak undershoot (US)			Setting time (ST)		
		Scenario			Scenario			Scenario		
		1	2	3	1	2	3	1	2	3
SSO	Δf_1	0.0007	0.0017	0.0008	-0.0094	-0.0083	-0.0096	7.67	9.97	10
	Δf_2	0.0010	0.0036	0.0012	-0.0108	-0.0226	-0.0114	8.38	11.37	8.61

	Δf_3	0.0007	0.0078	0.0008	-0.0106	-0.0167	-0.0111	7.14	9.85	7.28
	ΔP_{tie12}	0.0008	0.0034	0.0010	-0.0003	-0.0020	-0.0003	12.23	8.91	2.68
	ΔP_{tie23}	0.0003	0.0124	0.0004	-0.0022	-0.0059	-0.0025	5.91	8.05	2.43
	ΔP_{tie13}	0.0019	0.0030	0.0016	-0.0003	-0.0011	-0.0003	4.51	8.23	2.76
DE	Δf_1	0.0021	0.0020	0.0022	-0.0154	-0.0138	-0.0156	11.10	11.17	11.28
	Δf_2	0.0022	0.0029	0.0023	-0.0138	-0.0222	-0.0144	10.79	12.37	10.81
	Δf_3	0.0023	0.0053	0.0024	-0.0163	-0.024	-0.0169	11.57	14.01	11.56
	ΔP_{tie12}	0.0001	0.0009	7.9×10-5	-0.0013	-0.0017	-0.0018	15.55	7.48	7.61
	ΔP_{tie23}	0.0008	0.0124	0.0008	-0.0029	-0.0066	-0.0033	7.49	10.48	10.04
	ΔP_{tie13}	0.0038	0.0060	0.0037	-0.0005	-0.0011	-0.0005	10.80	10.46	10.16
PSO	Δf_1	0.0135	0.0154	0.0139	-0.0186	-0.0190	-0.0188	26.81	31.62	31.56
	Δf_2	0.0132	0.0135	0.0135	-0.0225	-0.0253	-0.0231	26.90	31.39	31.36
	Δf_3	0.0070	0.0077	0.0071	-0.0229	-0.0236	-0.0233	25.55	25.82	25.59
	ΔP_{tie12}	0.0019	0.0095	0.0021	-0.0016	-0.0030	-0.00159	10.76	12.16	10.80
	ΔP_{tie23}	0.0140	0.0155	0.0145	-0.0074	-0.0080	-0.0076	21.64	21.48	21.71
	ΔP_{tie13}	0.0079	0.0092	0.0081	-0.0128	-0.0131	-0.0131	22.13	22.04	22.17

Table 5. Comparison of frequency deviation for different loading conditions

Ctrl.	%change in load	Δf_1			Δf_2			Δf_3		
		OS	US	ST	OS	US	ST	OS	US	ST
SSO	-50%	0.0002	-0.0061	7.46	0.0003	-0.0065	7.32	0.0002	-0.0067	7.75
	-25%	0.0004	-0.0077	7.93	0.0007	-0.0085	7.86	0.0005	-0.0085	8.31
	+25%	0.0010	-0.0111	10.59	0.0014	-0.0129	10.36	0.0010	-0.0125	10.95
	+50%	0.0012	-0.0128	10.79	0.0018	-0.0152	11.07	0.0013	-0.0145	10.87
DE	-50%	0.0011	-0.0100	9.66	0.00117	-0.0087	10	0.00116	-0.0108	11
	-25%	0.00163	-0.0127	10.31	0.00168	-0.0112	10.44	0.0017	-0.0135	8.91
	+25%	0.0026	-0.0179	11.81	0.0027	-0.0164	11.32	0.0028	-0.0191	11.72
	+50%	0.0031	-0.0206	12.18	0.0032	-0.0191	12.27	0.0034	-0.0219	11.83
PSO	-50%	0.0073	-0.0120	23.31	0.0071	-0.0145	23.18	0.0032	-0.014	24.50
	-25%	0.0104	-0.0152	30.94	0.0101	-0.0184	30.74	0.0051	-0.0186	25.27
	+25%	0.0167	-0.0218	31.83	0.0163	-0.0266	31.63	0.0088	-0.0272	30.15
	+50%	0.0199	-0.0252	32.06	0.0194	-0.03088	31.86	0.0107	-0.0315	30.70

Table 6. Tie line power deviation for different loading conditions

Ctrl.	%change in load	$\Delta P_{tie 12}$			$\Delta P_{tie 23}$			$\Delta P_{tie 13}$		
		OS	US	ST	OS	US	ST	OS	US	ST
SSO	-50%	0.0004	-0.0001	4.95	0.0001	-0.0013	4.52	0.0012	-0.0002	4.63
	-25%	0.0006	-0.0002	3.25	0.0002	-0.0017	3.11	0.0014	-0.0002	3.20
	+25%	0.0011	-0.0004	4.28	0.0004	-0.0027	6.97	0.0020	-0.0004	7.47
	+50%	0.0014	-0.0005	5.03	0.0005	-0.0031	7.60	0.0022	-0.0005	7.35
DE	-50%	0.00011	-0.0011	7.2	0.0004	-0.0017	5.43	0.0027	-0.00032	5.64
	-25%	6.8×10 ⁻⁵	-0.0012	7.42	0.0006	-0.0023	7.29	0.0033	-0.00042	5.80
	+25%	0.000120	-0.0013	7.66	0.00097	-0.0035	10.32	0.0043	-0.00063	10.41
	+50%	0.000123	-0.0015	7.75	0.00114	-0.0041	10.50	0.0048	-0.00073	10.63
PSO	-50%	0.0012	-0.00098	10.53	0.0087	-0.00413	18.6	0.0043	-0.0080	18.9
	-25%	0.0015	-0.0013	10.68	0.0113	-0.0057	18.61	0.0060	-0.0104	21.44
	+25%	0.00231	-0.0019	10.88	0.0166	-0.0091	22.21	0.0096	-0.0151	25.12
	+50%	0.00273	-0.0022	10.98	0.0194	-0.0108	29.26	0.0115	-0.0175	29.68

Table 7. Overshoot, undershoot and setting time of Δf_1 , Δf_2 , Δf_3 for different values of system parameters in scenario 1,2 and 3

System par.	%change	scen ario	Δf_1			Δf_2			Δf_3		
			OS	US	ST	OS	US	ST	OS	US	ST
T_t	-25%	1	0.0021	-0.014	11.43	0.0017	-0.013	11.51	0.0016	-0.015	12
		2	0.0019	-0.013	11.51	0.0016	-0.0203	11.44	0.0056	-0.0202	12

		3	0.0021	-0.0149	11.53	0.00176	-0.0137	11.56	0.00174	-0.015	12.10
T_r	+25%	1	0.00209	-0.0160	12.32	0.0035	-0.0145	19.09	0.0043	-0.017	28.55
		2	0.00301	-0.0143	15.58	0.0059	-0.023	28.77	0.0112	-0.0279	36.83
		3	0.0021	-0.0163	12.38	0.0036	-0.0152	19.17	0.0048	-0.0182	30.17
	-25%	1	0.0020	-0.0153	10.42	0.0023	-0.0138	10.36	0.0024	-0.0162	11.3
		2	0.0019	-0.0137	10.20	0.0030	-0.0221	9.98	0.0055	-0.024	13.98
		3	0.0021	-0.0155	10.58	0.0024	-0.0144	10.35	0.0026	-0.0169	11.32
T_{GH}	+25%	1	0.00212	-0.0153	11.54	0.00203	-0.0138	11.07	0.0021	-0.0163	11.72
		2	0.00197	-0.0138	11.79	0.00262	-0.0221	10.54	0.0051	-0.023	11.64
		3	0.0021	-0.0156	11.67	0.00207	-0.0144	11.13	0.0023	-0.0169	11.75
	-25%	1	0.00211	-0.0153	11.15	0.0021	-0.013	10.75	0.0022	-0.0163	11.53
		2	0.0019	-0.0138	11.3	0.0028	-0.0222	10.25	0.0053	-0.0239	14
		3	0.00217	-0.0156	11.3	0.00221	-0.0144	10.77	0.0024	-0.0169	11.56
T_{RS}	+25%	1	0.00214	-0.0153	11.08	0.0022	-0.0138	10.82	0.00229	-0.0163	11.59
		2	0.00197	-0.0137	11.04	0.00274	-0.022	10.34	0.0052	-0.023	11.52
		3	0.0022	-0.0156	11.27	0.00223	-0.0145	10.85	0.0024	-0.0169	11.62
	-25%	1	0.0022	-0.0153	11.04	0.00221	-0.0138	10.99	0.00224	-0.0162	11.7
		2	0.00197	-0.0137	11	0.0025	-0.0215	10.53	0.0051	-0.0233	11.67
		3	0.0022	-0.015	11.21	0.0022	-0.014	10.98	0.0024	-0.0160	11.73
T_{RH}	+25%	1	0.00206	-0.0153	11.24	0.00219	-0.0138	10.57	0.0023	-0.0163	11.39
		2	0.0019	-0.0138	11.6	0.0031	-0.0227	12.57	0.0054	-0.024	14.07
		3	0.0021	-0.0156	11.39	0.0022	-0.0144	10.59	0.0025	-0.017	11.43
	-25%	1	0.0021	-0.015	9.70	0.0029	-0.0139	10.17	0.0032	-0.0166	15.79
		2	0.0025	-0.0138	9.73	0.0049	-0.023	17.52	0.0074	-0.025	20.99
		3	0.0022	-0.015	9.76	0.0029	-0.014	12.57	0.0035	-0.0173	17.44
+25%	1	0.0020	-0.015	12.23	0.0018	-0.013	11.98	0.0019	-0.016	12.08	
	2	0.0018	-0.0137	12.26	0.0019	-0.021	12.45	0.0053	-0.0228	11.69	
	3	0.0020	-0.015	12.36	0.0018	-0.014	12.13	0.0020	-0.016	12.16	

Table 8. Overshoot, undershoot and setting time of $\Delta P_{tie 12}$, $\Delta P_{tie 23}$, $\Delta P_{tie 13}$ for different values of system parameters in scenario 1,2 and 3

System par.	%change	scenario	$\Delta P_{tie 12}$			$\Delta P_{tie 23}$			$\Delta P_{tie 13}$		
			OS	US	ST	OS	US	ST	OS	US	ST
T_t	-25%	1	8.75×10^{-5}	-0.0011	7.77	0.0005	-0.0026	7.70	0.0036	-0.0004	6.21
		2	0.0003	-0.001	7.42	0.001	-0.0053	7.57	0.0051	-0.0005	6.13
		3	7.81×10^{-5}	-0.00094	7.82	0.00056	-0.003	7.95	0.0035	-0.00041	6.25
	+25%	1	0.0004	-0.0014	7.57	0.0017	-0.0032	16.68	0.0040	-0.00116	13.61
		2	0.00143	-0.0026	12.15	0.0048	-0.0078	27.87	0.0066	-0.0031	26.12
		3	0.00034	-0.00148	7.59	0.00185	-0.0036	18.11	0.0039	-0.0012	16.55
T_r	-25%	1	4.95×10^{-5}	-0.00122	7.52	0.0009	-0.0029	10.05	0.0038	-0.00055	10.02
		2	0.0008	-0.0015	7.35	0.0025	-0.0065	10.39	0.0059	-0.0012	10.32
		3	6.49×10^{-5}	-0.00109	7.55	0.00096	-0.0033	10.14	0.0037	-0.00057	10.07
	+25%	1	9.89×10^{-5}	-0.00132	7.64	0.00073	-0.0029	7.45	0.0038	-0.00049	6.03
		2	0.00085	-0.0017	7.58	0.0025	-0.0064	10.46	0.0058	-0.0009	10.51
		3	9.84×10^{-5}	-0.0012	7.68	0.00079	-0.0033	7.52	0.0037	-0.00051	10.1
T_{GH}	-25%	1	7.77×10^{-5}	-0.0013	7.54	0.00079	-0.0029	7.45	0.0038	-0.00052	10.05
		2	0.0008	-0.0018	7.46	0.0026	-0.0065	10.39	0.0059	-0.001	10.43
		3	7.82×10^{-5}	-0.0012	7.59	0.00085	-0.0033	10.04	0.0037	-0.0005	10.14
	+25%	1	8.03×10^{-5}	-0.00125	7.60	0.00081	-0.0029	7.50	0.0038	-0.0005	10.13

		2	0.00085	-0.0017	7.49	0.0025	-0.0065	10.47	0.0059	-0.001	10.50
		3	8.03×10^{-5}	-0.0011	7.64	0.00087	-0.0033	10.05	0.0037	-0.0005	10.22
T_{RS}	-25%	1	8.85×10^{-5}	-0.0011	7.72	0.00081	-0.0029	7.67	0.0038	-0.00051	10.16
		2	0.0007	-0.0014	7.56	0.0022	-0.0055	10.49	0.0058	-0.001	10.57
		3	8.38×10^{-5}	-0.00101	7.75	0.00086	-0.0033	7.70	0.0037	-0.00053	10.28
	+25%	1	7.91×10^{-5}	-0.0014	7.42	0.0008	-0.0029	9.95	0.0038	-0.0005	10.01
		2	0.001	-0.002	7.41	0.0029	-0.0065	10.37	0.0084	-0.0011	10.34
		3	8.18×10^{-5}	-0.00135	7.48	0.00087	-0.0033	10.1	0.0037	-0.0005	10.08
T_{RH}	-25%	1	0.00043	-0.0015	7.34	0.0013	-0.003	10.55	0.0038	-0.0008	10.53
		2	0.0013	-0.0028	11.91	0.0043	-0.0065	16.78	0.0062	-0.00208	13.74
		3	0.0004	-0.0016	7.34	0.0014	-0.0034	10.56	0.0037	-0.0009	10.55
	+25%	1	3.75×10^{-5}	-0.0012	7.76	0.00061	-0.0028	7.39	0.0038	-0.0003	5.78
		2	0.0005	-0.0012	7.50	0.0018	-0.0055	10.11	0.0057	-0.0007	5.76
		3	5.21×10^{-5}	-0.0009	7.86	0.00066	-0.0033	7.51	0.0037	-0.0003	5.84

References

- [1] A. Davidson, S. Ushakumari, Optimal load frequency controller for a deregulated non-reheat thermal power system, Control Communication & Computing India (ICCC), 2015 International Conference on, IEEE, 2015, pp. 319-324.
- [2] B. Hobbs, Linear complementarity models of Nash-Cournot competition in bilateral and POOLCO power markets, IEEE Transactions on power systems, 16 (2001) 194-202.
- [3] H. Bevrani, Y. Mitani, K. Tsuji, Robust decentralized AGC in a restructured power system, Energy Conversion and management, 45 (2004) 2297-2312.
- [4] P. Kumar, D.P. Kothari, Recent philosophies of automatic generation control strategies in power systems, IEEE transactions on power systems, 20 (2005) 346-357.
- [5] F. Liu, Y. Song, J. Ma, S. Mei, Q. Lu, Optimal load-frequency control in restructured power systems, IEE Proceedings-Generation, Transmission and Distribution, 150 (2003) 87-95.
- [6] V. Donde, M. Pai, I.A. Hiskens, Simulation and optimization in an AGC system after deregulation, IEEE transactions on power systems, 16 (2001) 481-489.
- [7] H. Shayeghi, A. Jalili, H. Shayanfar, Robust modified GA based multi-stage fuzzy LFC, Energy Conversion and Management, 48 (2007) 1656-1670.
- [8] M. Deepak, R.J. Abraham, Load following in a deregulated power system with thyristor controlled series compensator, International Journal of Electrical Power & Energy Systems, 65 (2015) 136-145.
- [9] B.K. Sahu, S. Pati, S. Panda, Hybrid differential evolution particle swarm optimisation optimised fuzzy proportional-integral derivative controller for automatic generation control of interconnected power system, IET Generation, Transmission & Distribution, 8 (2014) 1789-1800.
- [10] M. Ponnusamy, B. Banakara, S.S. Dash, M. Veerasamy, Design of integral controller for load frequency control of static synchronous series compensator and capacitive energy source based multi area system consisting of diverse sources of generation employing imperialistic competition algorithm, International Journal of Electrical Power & Energy Systems, 73 (2015) 863-871.
- [11] A.A. El-Fergany, M.A. El-Hameed, Efficient frequency controllers for autonomous two-area hybrid microgrid system using social-spider optimiser, IET Generation, Transmission & Distribution, 11 (2017) 637-648.
- [12] A. Zaidi, Q. Cheng, Online and offline load frequency controller design, Power and Energy Conference (TPEC), IEEE Texas, IEEE, 2017, pp. 1-6.
- [13] T. Yang, H. Cimen, Q. Zhu, Decentralised load-frequency controller design based on structured singular values, IEE Proceedings-Generation, Transmission and Distribution, 145 (1998) 7-14.
- [14] P. Babahajiani, Q. Shafiee, H. Bevrani, Intelligent demand response contribution in frequency control of multi-area power systems, IEEE Transactions on Smart Grid, 9 (2018) 1282-1291.
- [15] V. Gholamrezaie, M.G. Dozein, H. Monsef, B. Wu, An optimal frequency control method through a dynamic load frequency control (LFC) model incorporating wind farm, IEEE Systems Journal, 12 (2018) 392-401.
- [16] H. Alhelou, M.-E. Hamedani-Golshan, R. Zamani, E. Heydarian-Forushani, P. Siano, Challenges and Opportunities of Load Frequency Control in Conventional, Modern and Future Smart Power Systems: A Comprehensive Review, Energies, 11 (2018) 2497.
- [17] H. Shabani, B. Vahidi, M. Ebrahimpour, A robust PID controller based on imperialist competitive algorithm for load-frequency control of power systems, ISA transactions, 52 (2013) 88-95.
- [18] A.S. Meliopoulos, G.J. Cokkinides, A. Bakirtzis, Load-frequency control service in a deregulated environment, Decision Support Systems, 24 (1999) 243-250.

- [19] H. Shayeghi, H. Shayanfar, O. Malik, Robust decentralized neural networks based LFC in a deregulated power system, *Electric Power Systems Research*, 77 (2007) 241-251.
- [20] S.B. Shree, N. Kamaraj, Hybrid neuro fuzzy approach for automatic generation control in restructured power system, *International Journal of Electrical Power & Energy Systems*, 74 (2016) 274-285.
- [21] W. Tasnin, L.C. Saikia, M. Raju, Deregulated AGC of multi-area system incorporating dish-Stirling solar thermal and geothermal power plants using fractional order cascade controller, *International Journal of Electrical Power & Energy Systems*, 101 (2018) 60-74.
- [22] N. Kumar, B. Tyagi, V. Kumar, Application of fractional order PID controller for AGC under deregulated environment, *International Journal of Automation and Computing*, 15 (2018) 84-93.
- [23] G. Mahesh, P. Dewangan, Implementation of 2-DOFPID controller in multi area deregulated power system, 2018 Second International Conference on Inventive Communication and Computational Technologies (ICICCT), IEEE, 2018, pp. 1898-1903.
- [24] G.C. Sekhar, R.K. Sahu, A. Baliarsingh, S. Panda, Load frequency control of power system under deregulated environment using optimal firefly algorithm, *International Journal of Electrical Power & Energy Systems*, 74 (2016) 195-211.
- [25] Y.K. Bhatshvar, H. Mathur, Frequency Stabilization for Thermal-Hydro Power System with Fuzzy Logic Controlled SMES Unit in Deregulated Environment, *Advanced Computing & Communication Technologies (ACCT)*, 2014 Fourth International Conference on, IEEE, 2014, pp. 536-540.
- [26] O. Abedinia, Mohammad. S. Naderi, A. Ghasemi, Robust LFC in Deregulated Environment: Fuzzy PID using HBMO, *Proceeding of the IEEE International Power & Energy Society Power Systems Conference and Exposition, Italy, Rome (IEEEIC)*, 2011, pp. 74-77.
- [27] O. Abedinia, N. Amjady, M.S. Naderi, Multi-stage Fuzzy PID Load Frequency Control via SPHBMO in deregulated environment, *Environment and Electrical Engineering (EEEIC)*, 2012 11th International Conference on, IEEE, 2012, pp. 473-478.
- [28] R.K. Sahu, S. Panda, U.K. Rout, DE optimized parallel 2-DOF PID controller for load frequency control of power system with governor dead-band nonlinearity, *International Journal of Electrical Power & Energy Systems*, 49 (2013) 19-33.
- [29] P. Hota, B. Mohanty, Automatic generation control of multi source power generation under deregulated environment, *International Journal of Electrical Power & Energy Systems*, 75 (2016) 205-214.
- [30] S. Abd-Elazim, E. Ali, Load frequency controller design of a two-area system composing of PV grid and thermal generator via firefly algorithm, *Neural Computing and Applications*, 30 (2018) 607-616.
- [31] T.S. Gorripotu, R.K. Sahu, S. Panda, Firefly algorithm optimised PID controller for automatic generation control with redox flow battery, *International Journal of Computational Systems Engineering*, 3 (2017) 48-57.
- [32] K. Chandrasekar, B. Paramasivam, I. Chidambaram, Ancillary Service Requirement Assessment Indices for the Load Frequency Control in a Restructured Power System with Redox Flow Batteries, *Journal of Electrical Engineering & Technology*, 11 (2016) 1535-1547.
- [33] P. Bhatt, R. Roy, S. Ghoshal, Optimized multi area AGC simulation in restructured power systems, *International Journal of Electrical Power & Energy Systems*, 32 (2010) 311-322.
- [34] S. Anbarasi, S. Muralidharan, Hybrid BFPSO approach for effective tuning of PID controller for load frequency control application in an interconnected power system, *Journal of Electrical Engineering & Technology*, 12 (2017) 1027-1037.
- [35] M.-S. Park, Y.-H. Chun, Introduction of Generator Unit Controller and Its Tuning for Automatic Generation Control in Korean Energy Management System (K-EMS), *Journal of Electrical Engineering and Technology*, 6 (2011) 42-47.
- [36] J. James, V.O. Li, A social spider algorithm for global optimization, *Applied Soft Computing*, 30 (2015) 614-627.
- [37] E. Cuevas, M. Cienfuegos, D. Zaldívar, M. Pérez-Cisneros, A swarm optimization algorithm inspired in the behavior of the social-spider, *Expert Systems with Applications*, 40 (2013) 6374-6384.
- [38] S. Garcia, J. Luengo, F. Herrera, *Data Preprocessing in Data Mining*, Vol. 72 of Intelligent Systems Reference Library, Springer, 2015.
- [39] B. Tyagi, S. Srivastava, A decentralized automatic generation control scheme for competitive electricity markets, *IEEE transactions on power systems*, 21 (2006) 312-320.
- [40] S. Ajithapriyadarsini, P.M. Mary, M.W. Iruthayarajan, Automatic generation control of a multi-area power system with renewable energy source under deregulated environment: adaptive fuzzy logic-based differential evolution (DE) algorithm, *Soft Computing*, 1-15, 2019.